In-Situ Wear Measurement of Hot Forging Dies Using Robot Aided Endoscopic Fringe Projection

Philipp Middendorf[1,a*], Marcel Rothgänger[2,b], Julius Peddinghaus[2,c], Kai Brunotte[2,d], Johanna Uhe[2,e], Bernd-Arno Behrens[2,f], Lorenz Quentin[1,g], Markus Kästner[1,h], and Eduard Reithmeier[1,i]

[1]Leibniz Universität Hannover, Institute of Measurement and Automatic Control,

An der Universität 1, 30823 Garbsen, Germany

[2]Leibniz Universität Hannover, Institute of Forming Technology and Machines,

An der Universität 2, 30823 Garbsen, Germany

[a]philipp.middendorf@imr.uni − hannover.de , [b]m.rothgaenger@ifum.uni − hannover.de ,
[c]peddinghaus@ifum.uni − hannover.de , [d]brunotte@ifum.uni − hannover.de ,
[e]behrens@ifum.uni − hannover.de , [f]quentin@imr.uni − hannover.de ,
[g]markus.kaestner@imr.uni − hannover.de , [h]eduard.reithmeier@imr.uni − hannover.de

Abstract. According to the current state of the art, wear conditions of forging dies are assessed visually in the dismantled state, as there is no measuring procedure available for inline wear measurement of hot forging dies.

This paper introduces a handling concept for automated loading and in-situ tool inspection for a hot forging process. An industrial robot with a quick-change system mounted on its endeffector is utilized to integrate both, a high-temperature gripper and an endoscopic 3D-measurement sensor. By adapting the measuring method of fringe projection to an endoscopic design, the measuring system can be navigated into the difficult-to-access geometry of the forge and take high-precision 3D-measurements of the forging die. The ambient air heated by the forming process creates an inhomogeneous refractive index field around the measuring system and the hot die, which deflects the light during the measurement and deteriorates the overall accuracy of the reconstructed point cloud. This can lead to strong deviations in the reconstructed point clouds and the functional geometries calculated from them. Using a compressed air actuator, the measuring system can be protected from the heat effects of the measuring object, as well as from dirt. Furthermore, the effect of the inhomogeneous refractive index field can be significantly reduced. With this approach the in-situ wear measurement at highly stressed regions using the example of the mandrel radius and the flash radius will be demonstrated. These functional elements are of particular interest, as the thermal stress is high and large material flow takes place. For the wear determination, the functional elements of the tool are examined in detail by fitting geometrical features into the reconstructed point clouds and determining the deviations from a reference geometry. In addition, the measurement data is validated with the aid of a commercially available state-of-the-art measurement system.

Introduction

Forming is an economically viable manufacturing process for the production of components in large quantities [1]. When compared to other manufacturing processes, components made by bulk metal forming exhibit advantageous mechanical properties, such as increased fatigue strength [2]. Their increased load capacity results from the fiber flow that occurs during forming [3]. Furthermore, internal compressive stresses are induced, which make the components less prone to cracking [4]. Die forging can be assigned to compressive forming and has established itself industrially due to its wide range of applications. A distinction is made between cold, warm and hot forming. One of the main advantages of hot forming is the low force requirement, as heated billets exhibit a low flow stress [5]. However, hot forging tools are subject to high mechanical, thermal, tribological and chemical loads, that appear

superimposed, which results in a complex load spectrum [6]. From a long term point of view, the tools cannot withstand the loads without damage, which leads to various causes of tool failure. The most common causes of forging die failure are plastic deformation, cracks and wear [7]. Plastic deformation occurs mostly due to a thermal softening of the surface layer of forging dies as a result of the contact with the pre-heated steel billets at up to $1270\,°C$ [8]. In order to reduce the thermal load on the tool, cooling lubricants are often applied, which lead to alternating thermocyclic loading of the tool surface layer. The resulting tension and compressive stress are the main cause for thermal cracking. Mechanical cracks formed by overstressing the tools, which often occurs in areas of increased notch effect, such as abrupt transitions within the tool engraving [1]. The progressive loss of material of a solid body is defined as wear [9]. It is significantly influenced by the hardness of the surface layer of the die, in consequence the thermal softening of the surface layer does promote wear [10]. The progressive loss of material can be characterized by so-called wear-quantities where a distinction is made between one-, two- and three-dimensional wear-quantities. Whereby the maximum deviation from the nominal geometry describes the linear amount of wear, the area of a section through the worn component describes the planimetric amount of wear and the volumetric amount of wear describes the volume removed [11]. A distinction between direct and related wear measurement can be made, where the load duration, throughput or load path serve as a reference value for the related wear parameters [12].

Causes of Tool Failure in Forging

At the Institute of Forming Technology and Machines, various forging die models have been developed which, depending on the geometry and the process, locally favour different primary types of loads.
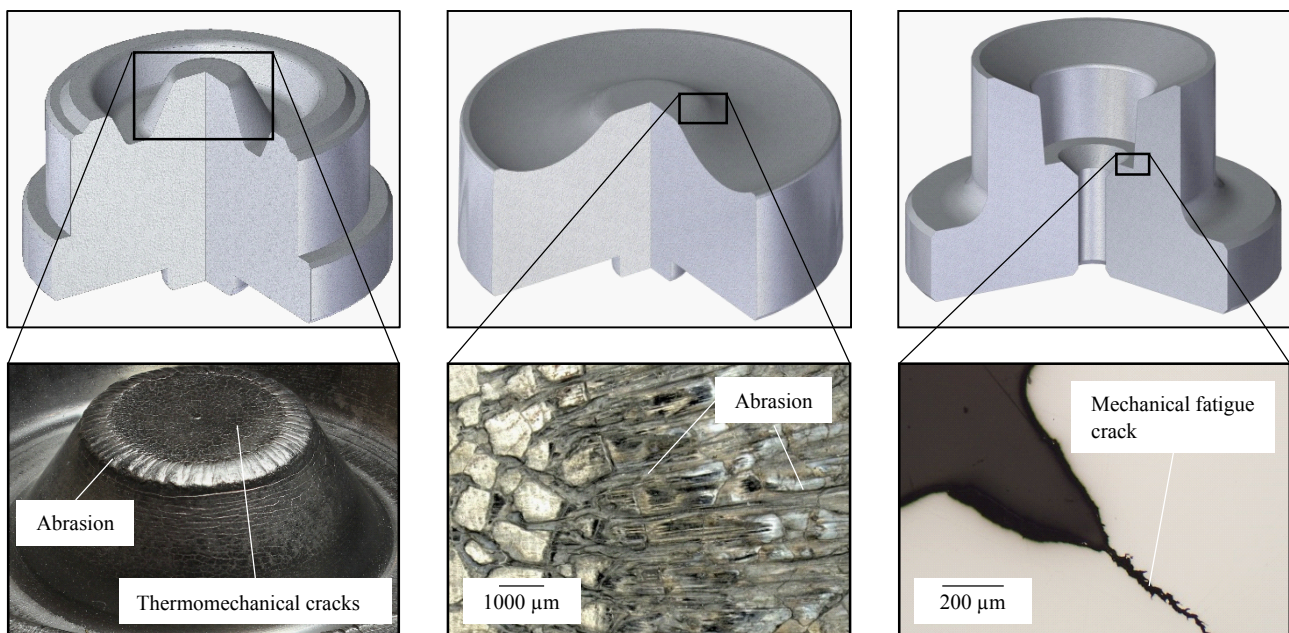

Fig. 1: Different primary types of load on model forging dies: (left) thermal, (centre) tribological and (right) mechanical [13].

Figure 1 (left) shows a forging die that is primarily subject to thermal loads in the area of the mandrel. During forming, the radius of the mandrel and the flank and centre are in contact with the billet. The billet is heated up to $1270\,°C$, which results in a high thermal load on the mandrel radius due to thermal accumulation. The surface layer of the radius is thermally softened, which increases abrasive wear. Furthermore, the plastic deformation in this area of the forging die is favoured because of the lowered hardness. The application of cooling lubricants reduces the thermal stress on the tool. The thermocyclic

alternating loads lead to changes in tensile and compressive stress that damages the surface layer, resulting in a fine network of cracks [13]. Figure 1 (centre) shows a forging die that is primarily subject to tribological loads. Due to the long flow path, abrasive wear dominates, which becomes apparent in form of material removal and grooves. The illustration shows a nitrided forging die. Due to the high hardness, there is an increased susceptibility to thermomechanical cracking, especially in the flat mandrel area. Figure 1 (right) shows a forging die, that is primarily subject to mechanical loads. An abrupt change in geometry of almost 90° can be seen on the base of the engraving, which creates a high notch effect and promotes mechanical fatigue cracking.

Measurement of Wear-Quantities on Forging Dies

Currently, commercially available optical measuring devices are used for the ex-situ determination of wear-quantities on forging dies, where the selection of the most suitable method depends on the focus of the investigation and the geometric dimensions. For measuring the dies in Figure 1 3D-profilometers, which are based on the fringe projection profilometry, can be used to measure the thermal or tribological loaded variants (e.g. Keyence Corporation (Osaka, Japan), type VR 3200). The forging dies are therefore measured in their initial state and after forging so that the tool conditions can be determined continuously and a deviation from the registered CAD geometry can be calculated. Surface profiles from both measurements can then be compared. The main advantage of this method is the precise determination of the linear and planimetric wear-quantities. However, due to the size of the 3D-profilometer, only small samples and tools can be measured. Furthermore, the analysis is limited to a previously defined focus area because the depth of field is not sufficient for greater height differences. For larger forging dies, a 3D-scanner, also based on fringe projection profilometry can be used (e.g. GOM GmbH a ZEISS company (Braunschweig, Germany), type ATOS Core 200). Due to the larger measurement volume, the 3D-scanner may have greater uncertainties than the 3D-profilometer. Alternative optical measuring methods suitable for the measurement of forging tools are the principle of focus variation and laser confocal scanning microscopes. The focus variation can achieve a higher reconstruction quality than fringe projection systems (e.g. Alicona Imaging GmbH (Graz, Austria), type InfiniteFocusG5), but is less accurate than the laser confocal scanning microscopes (e.g. Keyence Corporation, type VK-X3000 series). With increasing reconstruction accuracy, the measuring volume of the sensors decreases. Furthermore, the required measuring time increases and, depending on the specimens geometry, the desired magnification of the microscope cannot be used. Thus, the principle of fringe projection profilometry is the most flexible and robust measuring method for the application in the forge.

In the context of this study, the in-situ wear measurements during the forging process are carried out on a forging die that is primarily subject to thermal loads. As a result of the thermal influence, the mandrel radius is softened, increasing abrasive wear and plastic deformations. These two causes of failure are verified in-situ with the measurement system presented within this study. On the basis of an endoscopic fringe projection system, which was developed for 3D-measurement in confined spaces, the geometric condition characterisation of forging tools can be carried out. For this purpose, the handling concept used for the robot assisted in-situ measurement is explained, the optical measurement setup is introduced in detail, and the point cloud registration and wear determination are presented.

Handling Concept

In order to enable in-situ tool wear measurement, an efficient handling of the workpiece and the measuring system has to be realised. For this purpose, the high-temperature gripper from Figure 2 (left), which is used to equip the inductive heating device before and the forging press after heating up the forging billets, was adapted to an universal quick-change tool system. Similarly, the optical measuring system is also adapted to the interface of the quick-change system to enable uniform handling (see Figure 3).
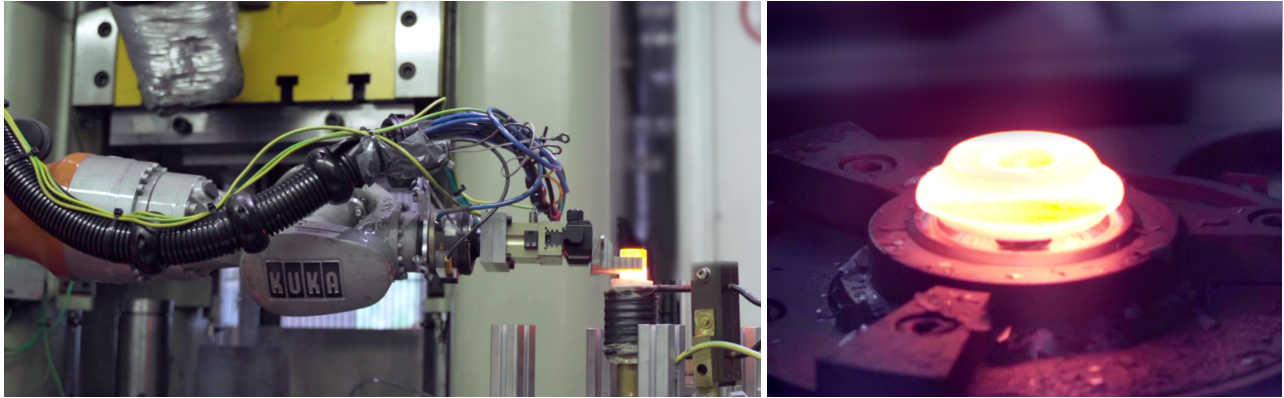
Fig. 2: Forge loading mechanism and forged components. (left) Conventional loading of the induction heater and forge with raw material (h = 40 mm, = 30 mm) by a robot-assisted high-temperature gripper. (right) Resulting formed workpiece.

Using the quick-change system SWS-007 / SWK-007 from SCHUNK GmbH & Co. KG (Lauffen/ Neckar, Germany), a repeatable coupling between the measuring system or gripper and the robot can be assured and the required media and signals such as compressed air, power supply and control signals are routed to the gripper or measuring system. The robot used, KR 16-2 F-S from KUKA Roboter GmbH (Gersthofen, Germany), offers a maximum payload of 16 kg and a repeatability accuracy of $\pm$ 0.05 mm. To allow the use of the fringe projection system in the forging environment, the optical measurement system must first be protected from dirt and external temperature influences. With a specially manufactured compressed air nozzle, both forging residues can be removed before measurement and a continuous cooling of the measuring head and the ambient air can be achieved.
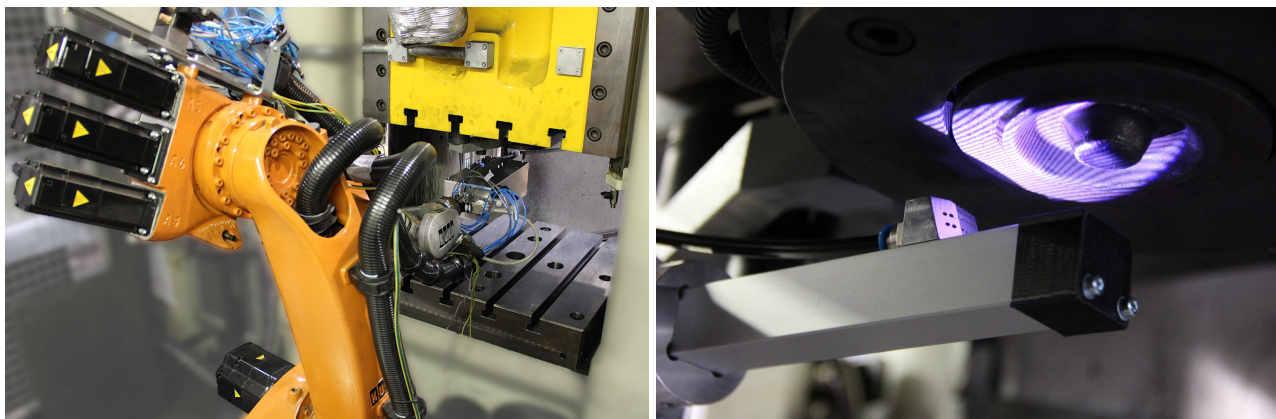

Fig. 3: Measurement of the forging tool with a robot-assisted endoscopic fringe projection system. (left) Clutching of the endoscopic fringe projection system to the robot by means of a quick tool change system. (right) Close-up of a fringe projection measurement of the upper die.

The heat input of the hot forging components (1270 °C) and tools (250 °C) causes an inhomogeneous refractive index field. This leads to light deflection effects that greatly increases the measurement uncertainty of optical measurement systems [14]. With the help of a compensation approach using compressed air actuators, it could already be shown that the impact of the inhomogeneous refractive index field can be reduced [15]. For this reason, an adapted multi-channel nozzle, which flows off at several angles, was developed. Figure 3 (left) shows the fundamental set-up of the handling concept at the press and the measuring system mounted on the robot in an exemplary measuring pose. In Figure 3 (right) an enclosure-protected measuring system during a fringe projection measurement of the upper

die is depicted. In order to integrate geometry measurement into the forming process, particularly short measurement and evaluation times are relevant. With the current measuring head, the measuring time is about 3 seconds per measuring pose for a single exposure time and about 10 seconds for a high dynamic range (HDR) measurement consisting of 3 exposure times. In the future, these times can be halved by the progressive miniaturization of industrial camera sensors and a better triggering capability of the sensor. For the evaluation of the 3D measurements, registration to CAD data and deviation analysis has to be performed. This takes currently about 15 seconds, so that the entire tool evaluation can be carried out within a few forging cycles.

Measurement Setup

An endoscopic measuring system based on the principle of the borescopic fringe projection was developed for high-precision 3D measurement in confined spaces [16], the basic function is illustrated in Figure 4. This instrument enables navigation into holes and cross-sections of less than $10\,mm$ diameter and can thus be applied for inspections in areas that are difficult to access. In the in-line forging process, such a miniaturized inspection system is essential to provide the required sensor positioning, as well as the necessary protective enclosures and mountings for the compressed air actuators. In particular, the measuring head designed for the upper die makes it possible to cover a field of view of $30\,mm$ x $40\,mm$ at a working distance of $40\,mm$ and thus to reconstruct the relevant areas of the die. Commercial fringe projection systems with larger working ranges are not able to meet these requirements, so that in-situ measurements can not be performed due to limited space inside of the forging process.
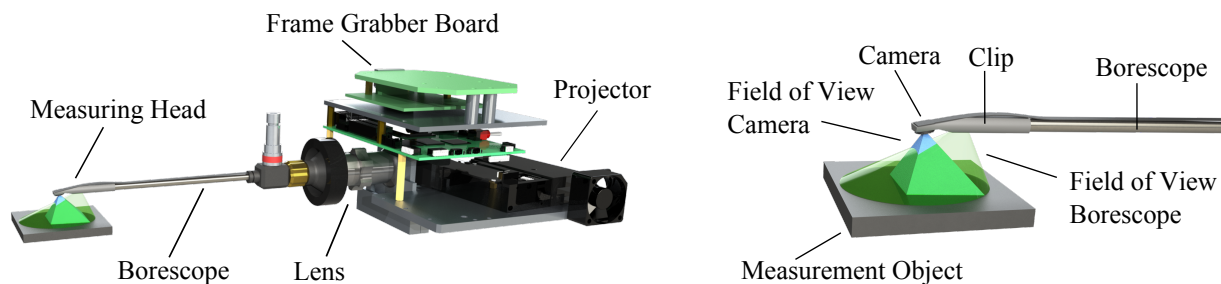

Fig. 4: Endoscopic fringe projection system. (left) Setup of a rigid endoscopic fringe projection system for the 3D-measurement in confined spaces. (right) Essential components and field of view of the measuring head of an endoscopic fringe projection sensor.

The principle of a rigid endoscopic fringe projection system enables the implementation of a modular and compact sensor head for high-precision 3D inspection, based on a miniature camera and boroscope as well as a projection unit and frame grabber board. A borescope based on the Hopkins rod-lens system with a diameter of $6.5\,mm$ and lengths of $300\,mm$ is used as the optical connection between the measuring head and the projector. Figure 4 (left) shows the main components of the camera and projection unit. A DLP 4500 EVM micromirror device supplied by Texas Instruments Inc (Dallas, US) forms the fringe pattern by binary tilting each individual micro mirror. A C-mount lens ($f = 38\,mm$) is used in order to couple the projection into the borescope and thus to image the structured light onto the measurement scene. The endoscope features a viewing direction of 70° and an aperture angle of 80°. On the camera side, a miniaturised 2-megapixel multimedia sensor OV2740 from the manufacturer OmniVision Technologies, Inc (Santa Clara, United States) in the MP-FPC31105-18350-200 version ($f = 1.83\,mm/F8.0$) from the manufacturer MISUMI Electronics Corp. (New Taipei, Taiwan) is applied. Figure 4 (right) shows the schematic function and the relevant components of the measuring head as well as the fields of view of the camera and borescope. By using a movable clip to align the camera on the borescope, the triangulation base of the sensor and thus the working distance of the

endoscope can be adjusted. Especially components of camera and endoscope are highly miniaturised, which lead to strong distortions of the captured images. Therefore, the camera is calibrated according to the pinhole approach of Zhang et al. using reference features of a dot grid, low reflection target [17]. In a further step, the projector is calibrated as an inverse camera. The radial and tangential distortion of camera and projector is calculated via the polynomial approach of Conrady and Brown [18]. Where the camera exhibits pincushion distortion, while the projector has a barrel distortion [19]. Finally, a stereo calibration of camera and projector is performed. Within the framework of the fringe projection measurements, a multi-frequency phase shift method is used for phase demodulation. To classify the reconstruction quality, the probing error with respect to form was determined to be 20 µm according to VDI/VDE 2634-2 [20] for a cylindrical feature of a calibrated microcontour standard with a measuring head at 30 mm working distance. The probing error with respect to size on this feature is 40 µm with 20 repeated measurements following the guideline JCGM 100:2008 [21]. According to the calibration certificate, the radius is 5994.0 µm. For further accuracy and measurement uncertainty investigations and supplementary explanations, please refer to [22]. For measurements on surfaces with limited optical cooperativity, the known physical limits of triangulating optical measurement principles apply.

Point Cloud Registration and Wear Determination

For point cloud registration and the calculation of deviations to the CAD models, the point clouds must first be pre-processed. For this purpose, an outlier removal is carried out using a Laplace filter and a resampling of the CAD model into a reference point cloud is realised. The reference point cloud is generated in order to implement subsequent alignments and distance determinations to the CAD geometry. This is followed by a manual pre-alignment, which can be replaced further on by a hand-eye calibration of the robot guided measurement system and the estimation of the kinematic chain. After a coarse pre-alignment of the data, a numerical fine adjustment is performed using the Iterative
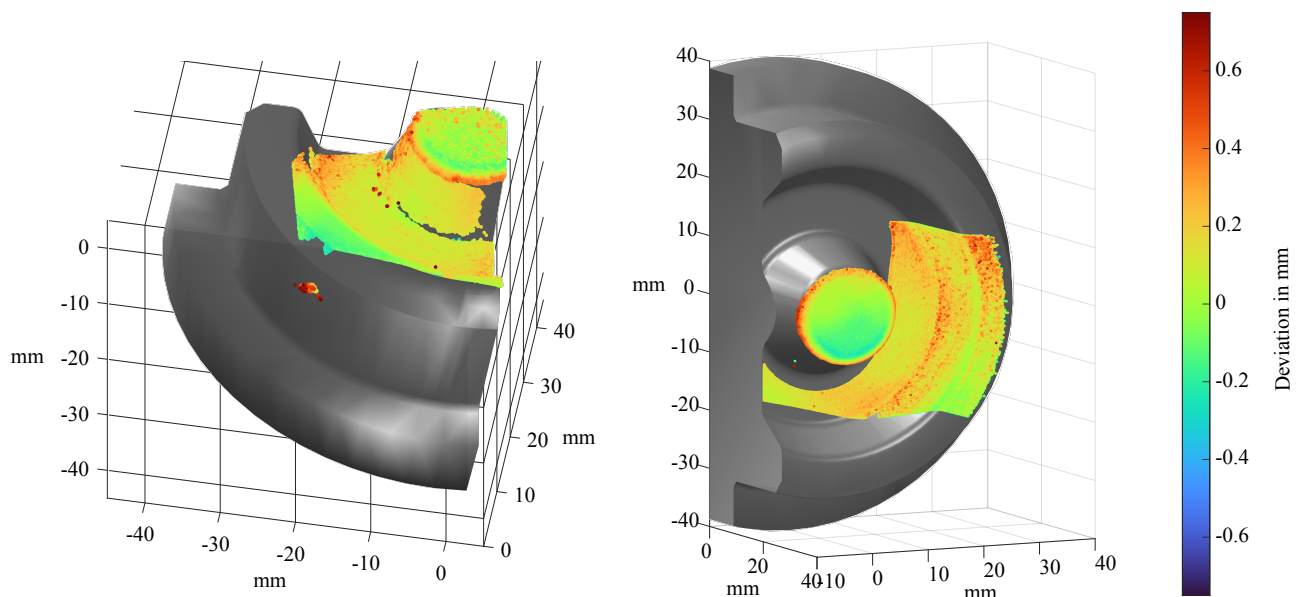

Fig. 5: Point deviations of the reconstructed fringe projection measurements of the endoscopic sensor to the CAD geometry. (left) Deviation map of the mandrel radius and the flank of the mandrel. (right) Deviation map of the top of the mandrel and the burr path radius.

Closest Point (ICP) algorithm [23, 24], which minimizes the point distances of all determined point correspondences. A detailed explanation of a similar data registration approach has been published by Hinz et al. [25]. After optimal registration respectively fitting, the deviation of the point cloud to

the CAD geometry is determined in polygonal normal direction. For the assignment of the respective (polygon) planes to the corresponding 3D points, a 1-NN classification of the reference point cloud (generated from all polygons) and the reconstructed point cloud is carried out first. Subsequently the point deviation of all points is determined to the nearest polygon. Figure 6 shows the registration result with subsequent determination of the deviation analysis from two endoscopic fringe projection measurements, whereby the left figure focuses on the mandrel radius and the flank of the stamp and the right figure shows the calculated deviations of the burr path radius. The calculated point deviations per point correspond to the linear wear amount according to the original definition of the standard DIN 50321 and can be used to quantify wear representing a direct wear parameter according to [11]. It has to be considered that, compared to the CAD geometry, a graphite spray with varying thickness is applied for the forging process. This leads to geometric changes and can possibly limit the detection of wear based on the reconstructed point clouds. To visualise the abrasive wear of the upper die due to the thermal load in the planimetric view, an exemplary sectional view is provided through the die with main focus on the mandrel radius in Figure 6 (left). A material shift over the mandrel radius towards the flank can be seen in the reconstructed endoscopic measurements. This is evident from the negative point deviation on the top of the die and the positive point deviation on the flank of the mandrel. At the lower radius of the section in Figure 6 (left), a deviation of the contour can be seen; this is due to a specular highlight and can be masked by means of a continuity criterion. By determining the area of the deviation from the nominal contour, the planimetric amount of wear can be calculated.

(a) Endoscopic measurement   (b) Reference measurement with GOM sensor
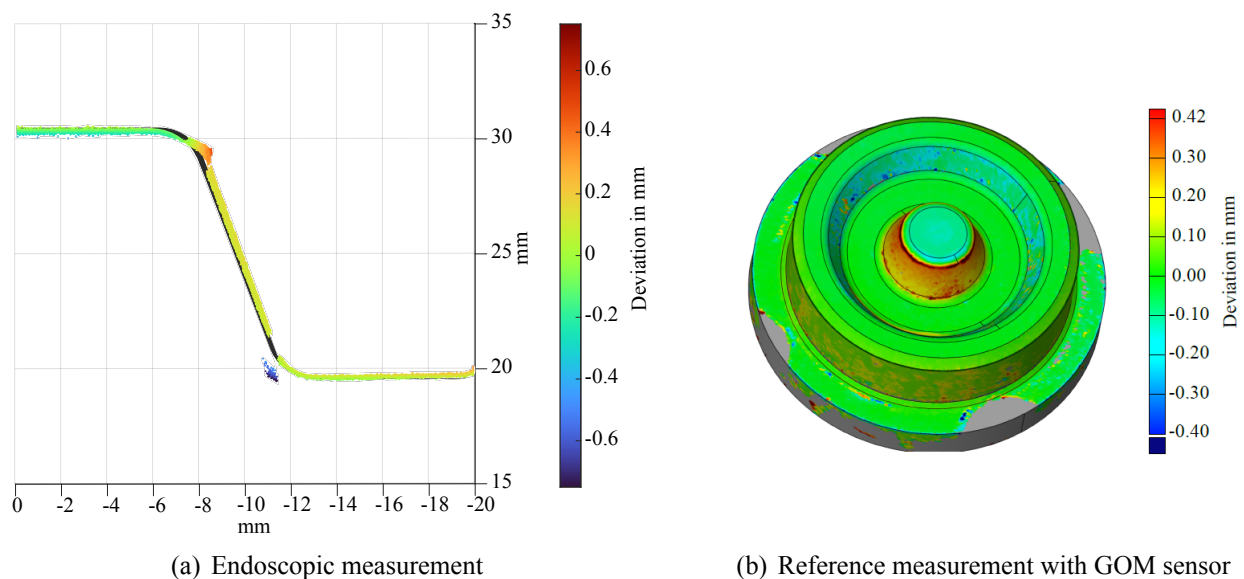
Fig. 6: Evaluated measurement data of the endoscopic sensor and the reference measurements. (left) Section through the contour of the endoscopic in-situ measurement. (right) Reference measurement of the dismantled tool using a commercial fringe projection system ATOS Core 200 (GOM GmbH).

In order to validate the suitability of the presented measuring system, the worn die is measured using an industrial fringe projection system (ATOS Core 200 from GOM GmbH). For this purpose, the die is measured in the dismantled state with 20 measuring poses and a surface comparison to the CAD geometry is carried out. Figure 6 (right) shows the resulting deviations. From a qualitative point of view, the reconstructed point clouds of the endoscopic sensor and the industrial sensor show a uniform inspection result. Each point cloud of the two sensors is registered separately on the parallel planes of the stamp top and base and show uniform deviations below $100\,\mu m$ to the CAD file. This indicates that tilting of the fitted planes is avoided. The application of graphite spray, the high noise of the miniaturised sensor [19], and the comparatively low lateral and axial resolution of $80\,\mu m$ [26] the industrial sensor (due to a large measurement volume) can lead to measurement deviations in this size range. In the area of the stamp flank symmetrical point deviations up to $200\,\mu m$ around the

stamp were determined with both sensors, therefore the alignment of the point clouds appears to be uniform, the influence of deviations due to registration is comparatively low and neglected in the further process. However, the measurement results of the endoscopic and industrial sensors cannot be compared quantitatively, as it is not possible to precisely align the measurements with each other without using additional reference features. During the measurement in the disassembled state, the measurement pose from the in-line process could not be identified due to unknown rotations of the die. Therefore no correct point correspondence can be established in both point clouds, which prevents a direct area comparison in the mandrel radius. To quantify the resolution of the endoscopic sensor, the nearest neighbour of all points in the filtered point cloud is identified based on the Euclidean distance. The lateral resolution is calculated using the Euclidean norm of the point distances with respect to the length and width and results in approximately 25 µm, see Figure 7. The axial resolution, determined by the Euclidean norm of the point distances in relation to the depth, cannot be determined representatively due to the planes in the sample geometry. It can be assumed to be in a similar size range. With increasing wear, the geometrical deviations of the forged parts increase gradually as well.
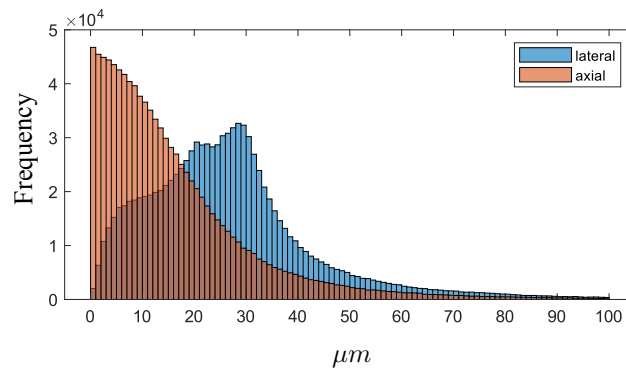

Fig. 7: Histogram of the lateral and axial resolution of the endoscopic sensor.

In the presented work, the serial forging tests are used to develop an in-situ measurement approach for the continuous progression of tool wear. The progression of wear can be monitored continuously between forging cycles throughout serial production with the developed endoscopic fringe projection sensor. By comparing the measured wear with the individual dimensional tolerances of the forged part, the wear status of the tool can be directly monitored to determine and predict the end-of life. In industrial applications however, the end-of-life criteria for forging tools are individual for each forging process, mainly depending on the geometrical requirements and dimensional tolerances for the forged parts which can vary immensely in different fields. In the presented experimental work, the forged parts merely serve the academic purpose of initiating wear for tool analysis. Therefore no specific geometry and dimension tolerance limits are given and the definition of an end-of-life criterion is not deducible, nor is it necessary, since the focus of this work lies on the development of continuous measurement of wear progress.

Conclusion and Future Work

The presented robot assisted handling concept for the loading and in-situ wear measurement enables a 3D-inspection for hot forming processes where inspection can be carried out between consecutive strokes of the forging process and has potential for resource savings through the avoidance of imperfect formed parts. The developed in-situ measuring method of robot-assisted endoscopic fringe projection enables the 3D measurement of forging tools, the calculation of geometric deviations and thus the quantification of abrasive wear. In particular, the point-by-point representation of the linear wear quantity enables the calculation of the planimetric and volumetric wear quantity as well as the related parameters using the reference parameters of load duration, throughput and load path, of the forging process.

In further experiments, the wear of the forming tool needs to be measured continuously with the presented measuring method in an automated forging process. Due to a constant alignment of the forging tool, a reproducible measuring pose can be achieved and the abrasive wear can be monitored and evaluated continuously over the lifetime of the die. Thus, in-situ wear measurements can be used to predict the expected tool life and thus enable better process planning by fitting tool life simulation models using this data. In addition, the application to tailored forming tools and work pieces is of particular interest, as both abrasive and adhesive wear occur and the effects on the forming process need to be investigated. In particular, the differentiation of the types of wear on the basis of fringe projection measurements is of interest.

Acknowledgments

References

[1] Buchmayr, B., "Damage, lifetime, and repair of forging dies," *BHM Berg- und Hüttenmännische Monatshefte* **162**, 88–93 (dec 2016).

[2] McKelvey, S. A. and Fatemi, A., "Surface finish effect on fatigue behavior of forged steel," *International Journal of Fatigue* **36**, 130–145 (mar 2012).

[3] Kumar, D. and Mondal, S., "A review on modelling, design and optimization of forging process," *IOP Conference Series: Materials Science and Engineering* **1126**, 012001 (mar 2021).

[4] Zhu, L. and Jia, M.-P., "A new approach for the influence of residual stress on fatigue crack propagation," *Results in Physics* **7**, 2204–2212 (2017).

[5] Totten, G., Funatani, K., and Xie, L., [*Handbook of Metallurgical Process Design*], Materials Engineering, CRC Press (2004).

[6] Hawryluk, M., Gronostajski, Z., Ziemba, J., Dworzak, Ł., Jabłoński, P., and Rychlik, M., "Analysis of the influence of lubrication conditions on tool wear used in hot die forging processes," *Eksploatacja i Niezawodnosc - Maintenance and Reliability* **20**, 169–176 (mar 2018).

[7] Abachi, S., Akkök, M., and Gökler, M. İ., "Wear analysis of hot forging dies," *Tribology International* **43**, 467–473 (jan 2010).

[8] Emamverdian, A. A., Sun, Y., and Chunping, C., "Deformation and wear in a h21 (3cr2w8v) steel die during hot forging: simulation, mechanical properties, and microstructural evolution," *Journal of Materials Research and Technology* **15**, 268–277 (nov 2021).

[9] Stachowiak, G. W., ed., [*Wear - Materials, Mechanisms and Practice*], John Wiley & Sons Ltd (nov 2005).

[10] Zwierzchowski, M., "Factors affecting the wear resistance of forging tools," *Archives of Metallurgy and Materials* **62**, 1567–1576 (sep 2017).

[11] Deutsches Institut für Normung e. V., "Din 50321 verschleiß-meßgrößen," Standard DIN 50321, Deutsches Institut für Normung e. V. (1997).

[12] Czichos, H. and Habig, K.-H., [*Tribologie-Handbuch*], Springer Fachmedien Wiesbaden (2015).

[13] Brunotte, K. and Behrens, B.-A., [*Beitrag zur Steigerung der Standmenge von Werkzeugen der Warmmassivumformung durch den Einsatz lokaler belastungsangepasster Verschleißschutzbehandlungen*], TEWISS Verlag, Garbsen (2021).

[14] Beermann, R., Quentin, L., Stein, G., Reithmeier, E., and Kästner, M., "Full simulation model for laser triangulation measurement in an inhomogeneous refractive index field," *Optical Engineering* **57**, 1 (nov 2018).

[15] Quentin, L., Reinke, C., Beermann, R., Kästner, M., and Reithmeier, E., "Design, setup, and evaluation of a compensation system for the light deflection effect occurring when measuring wrought-hot objects using optical triangulation methods," *Metals* **10**(7) (2020).

[16] Schlobohm, J., Pösch, A., Kästner, M., and Reithmeier, E., "On the development of a low-cost rigid borescopic fringe projection system," in [*Photonics, Devices, and Systems VI*], SPIE (Jan. 2015).

[17] Zhang, Z., "A flexible new technique for camera calibration," *IEEE Transactions on Pattern Analysis and Machine Intelligence* **22**(11), 1330–1334 (2000).

[18] Brown, D., "Close-range camera calibration," *Photogramm. Eng.* **37** (12 2002).

[19] Middendorf, P., Hedrich, K., Kästner, M., and Reithmeier, E., "Miniaturization of borescopic fringe projection systems for the inspection in confined spaces: a methodical analysis," in [*Emerging Digital Micromirror Device Based Systems and Applications XIII*], Lee, B. L. and Ehmke, J., eds., SPIE (mar 2021).

[20] Deutsches Institut für Normung e. V., "DIN 26343-2 Optical 3-D measuring systems, Optical systems based on area scanning," standard, Deutsches Institut für Normung e. V. (2012).

[21] International Organization for Standardization, "ISO/IEC GUIDE 98-3:2008, Uncertainty of measurement – Part 3: Guide to the expression of uncertainty in measurement (GUM:1995)," standard, International Organization for Standardization (2008).

[22] Matthias, S., Schlobohm, J., Kästner, M., and Reithmeier, E., "Fringe projection profilometry using rigid and flexible endoscopes," *tm - Technisches Messen* **84** (01 2017).

[23] Chen, Y. and Medioni, G. G., "Object modelling by registration of multiple range images," *Image Vis. Comput.* **10**, 145–155 (1992).

[24] Besl, P. and McKay, N. D., "A method for registration of 3-d shapes," *IEEE Transactions on Pattern Analysis and Machine Intelligence* **14**(2), 239–256 (1992).

[25] Hinz, L., Kästner, M., and Reithmeier, E., "Metal forming tool monitoring based on a 3d measuring endoscope using CAD assisted registration," *Sensors* **19**, 2084 (may 2019).

[26] Hinz, L., Metzner, S., Müller, P., Schulte, R., Besserer, H.-B., Wackenrohr, S., Sauer, C., Kästner, M., Hausotte, T., Hübner, S., Nürnberger, F., Schleich, B., Behrens, B.-A., Wartzack, S., Merklein, M., and Reithmeier, E., "Fringe projection profilometry in production metrology: A multi-scale comparison in sheet-bulk metal forming," *Sensors* **21**(7) (2021).